

Spin-Orbit Evolution of Short Period Planets

Ian Dobbs-Dixon¹, D.N.C. Lin^{1,2}, and Rosemary A. Mardling^{1,3}

1) *Department of Astronomy & Astrophysics, University of California, Santa Cruz, CA 95064, USA*

2) *Institute of Astronomy, Cambridge University, Cambridge CB3 0HA, UK*

3) *School of Mathematical Sciences, Monash University, Melbourne 3800, Australia*

`iandd@ucolick.org`, `lin@ucolick.org`, `rosemary.mardling@sci.monash.edu.au`

ABSTRACT

The negligible eccentricity of all extra solar planets with periods less than six days can be accounted for by dissipation of tidal disturbances within their envelopes which are induced by their host stars. In the period range of 7-21 days, planets with circular orbits coexist with planets with eccentric orbits. These will be referred to as the *borderline planets*. We propose that this discrepancy can be attributed to the variation in spin-down rates of young stars. In particular, prior to spin-down, dissipation of a planet's tidal disturbance within the envelope of a sufficiently rapidly spinning star can excite eccentricity growth, and for a more slowly spinning star, at least reduce the eccentricity damping rate. In contrast, tidal dissipation within the envelope of a slowly spinning low-mass mature star can enhance the eccentricity damping process. Based on these results, we suggest that short-period planets around relatively young stars may have a much larger dispersion in eccentricity than those around mature stars. We also suggest that because the rate of angular momentum loss from G and K dwarfs via stellar winds is much faster than the tidal transfer of angular momentum between themselves and their very-short (3-4 days) period planets, they cannot establish a dynamical configuration in which the stellar and planetary spins are approximately parallel and synchronous with the orbital frequency. In principle, however, such configurations may be established for planets (around G and K dwarfs) with orbital periods of up to several weeks. In contrast to G and K dwarfs, the angular momentum loss due to stellar winds is much weaker in F dwarfs. It is therefore possible for synchronized short-period planets to exist around such stars. The planet around Tau Boo is one such example.

1. Introduction

Radial velocity surveys around nearby solar-type stars have led to the discovery of planets with short-period and highly eccentric orbits (Marcy *et al.* 2000). The period distribution is essentially logarithmic ranging from a few days to many years. While the upper range of the period distribution at this stage is incomplete due to relatively short survey times, there is a minimum cutoff at around period $P = 3$ days. The observed eccentricities, e , of planets with $P > 21$ days are uniformly distributed in the range zero to about 0.7. However, all planets with $P < 6$ days have nearly circular orbits (Figure 1(a)). In this paper, we consider the effect of star-planet tidal interactions on the eccentricity distribution of the short-period planets (hot Jupiters).

The dichotomy in the planets’ eccentricity distribution is similar to that of binary stars (Mathieu 1994). It is generally assumed that the orbital eccentricities of binary stars with periods less than some critical value (the circularization period P_c) are damped by their tidal interaction (Zahn 1977). The magnitude of P_c is a function of the tidal dissipation efficiency and the age of the binary. The former quantity is usually parameterized in terms of the stars’ Q_* -values (cf Murray & Dermott 1999; in what follows, an asterisk subscript will refer to stellar values while the subscript p will refer to planets). Based on the observed magnitude of P_c in various stellar clusters (Mathieu 1994), the inferred values of $Q'_* = 3Q/2k_*$ (where k_* is the tidal Love number or twice the apsidal motion constant) are $\sim 1.5 \times 10^5$ (with $P_c \sim 4$ days) for young stars with age $\tau_* < 10^8$ yr, and $\sim 10^6$ for mature stars (Terquem *et al.* 1998).

The circularization of short-period planetary orbits may also be due to tidal dissipation processes (Rasio *et al.* 1996, Marcy *et al.* 1997). For example, this would be necessary to account for the small eccentricities of short-period planets if they were scattered into the vicinity of their host stars by other planets (Rasio & Ford 1996, Murray *et al.* 1998). In contrast, if short-period planets acquired their small semi-major axes through tidal interaction with their nascent disks (Lin *et al.* 1996), planet-disk resonant interactions would naturally damp the eccentricities of planets with masses $M_p < 10M_J$ (where M_J is the mass of Jupiter) (Goldreich & Tremaine 1980, Artymowicz 1992, Papaloizou *et al.* 2001) although in some circumstances, it may also excite planets’ eccentricities (Goldreich & Sari 2003). The processes (planet-star tidal interaction, unipolar induction, and disk depletion) which halted the orbital migration of hot Jupiters (Lin *et al.* 1996) may also induce the excitation of orbital eccentricity. In either early dynamical evolution scenarios, efficient post-formation eccentricity damping is needed to account for the small eccentricities (< 0.1) of the short-period planets.

The orbital semi-major axes of short-period planets are larger than the radii of their

host stars by an order of magnitude and of their own radii by two orders of magnitude. The angular momenta of these planetary orbits are comparable to that carried by the spin of their host stars and larger than that contained in their own spins. Unless their orbits are synchronized and circularized, these planets are subject to intense tidal disturbances from their host stars. The Q_p -value for Jupiter has been inferred from Io’s orbital evolution such that $5 \times 10^4 < Q'_p < 2 \times 10^6$ (Yoder and Peale 1981). With this range for Q'_p , planets with periods less than 6 days whose masses and radii are comparable to those of Jupiter are circularized during the main sequence lifetime ($\tau_* \sim$ a few Gyr) of solar-type dwarf stars. This estimate is consistent with the observed circular orbits of the shortest period planets (Trilling 2000).

The dissipation of these disturbances leads not only to dynamical changes but also to internal heating which may cause them to inflate (Bodenheimer *et al.* 2001). With a sufficiently large eccentricity, hot Jupiters would undergo runaway tidal inflation and overflow their Roche lobes before their orbits became circularized (Gu *et al.* 2003, 2004). Mass loss through Roche lobe overflow may either totally disrupt the planet or induce the orbital semi-major axis, a , to expand (Trilling *et al.* 1998). Both outcomes inhibit protoplanets from becoming too close to their host stars. Thus, the excitation and damping of eccentricity also has observable consequences and important implications for the structure and survival of individual planets and the period distribution of planetary systems.

The observed eccentricity distribution also indicates that planets with periods between 1 and 3 weeks have non-negligible eccentricities which are smaller than those of planets with longer periods and larger than those of planets with shorter periods. We will refer to planets in this period range as *borderline planets*. In this paper, we adopt a conventional approach using frequency independent $Q'_{p,*}$ -values to analyze the orbital evolution of a star-planet system (Mardling & Lin 2002).

In §2, we show that the observationally inferred eccentricities of these borderline planets are not well correlated with the expected time scale, τ_{ep} , for eccentricity damping due to the dissipation of the stellar tidal disturbance inside the planets. Although it is customary to assume that dissipation inside a planet provides the dominant contribution to its orbital eccentricity evolution, dissipation within its host star can have a comparable effect if $Q'_* \sim Q'_p$. We examine the possibility that, in this limit, the dispersion in the $(e-\tau_{ep})$ relationship is caused by the observed spread in stellar rotation rates. Stellar spin evolves as a consequence of structural changes within a star, as well as mass loss and tidal interaction with a planet.

In §3, we consider how these effects combined affect the long term evolution of a star’s spin as well as the eccentricity of a planetary orbit. We show that short-period planets rapidly evolve into a spin-orbit quasi-equilibrium which continues to evolve, albeit at a

slower pace, because the dissipation of the stellar tidal disturbance within a planet continues to induce eccentricity damping. In contrast, during the early stages of its main sequence evolution, a solar-type star rotates rapidly and is likely to excite the eccentricity of its planet. However, as it loses angular momentum and attains a modest or slow spin frequency, the tidal dissipation within such a star will induce eccentricity damping. We also deduce the condition for quasi-equilibrium in which the loss of angular momentum through a stellar wind is balanced by that transferred to a star through its tidal interaction with a short-period planet. We then explore the possibility of such a system evolving into a state in which the stellar and planetary spins are aligned, and the planet and the envelope of the star spin synchronously with the orbit. Finally in §4 we summarize our results and discuss their implications for the dynamical evolution of short-period planets and the spin-down history of their host stars.

2. The Eccentric Short-Period Planets

Observational determinations of planetary eccentricities require extremely accurate radial velocity data over many orbits. Spurious determinations of periods and eccentricities may be caused by sparse sampling, modest velocity measurement errors, and perturbations by other planets. Neglecting these potential sources of error in the published data, we find that half of the known systems with $1 \text{ week} < P < 3 \text{ weeks}$ have non negligible eccentricities. (We consider the present threshold of real detection to be $e = 0.1$ which corresponds to the typical ratio of residual to amplitude of radial velocity curves.) In this section, we consider the implications of these measurements.

2.1. Dispersion in the Eccentricity Evolution of Short-Period Planets

Using the standard formula (Goldreich & Soter 1966, Yoder & Peale 1981, Peale 1999, Murray & Dermott 1999, for the limitation and uncertainties see §1), the timescale associated with eccentricity damping due to dissipation of the stellar tidal disturbance in a planet can be expressed as

$$\tau_{ep} = -\frac{e}{\dot{e}} = \frac{4}{63} \frac{M_p}{M_*} \left(\frac{a}{R_p}\right)^5 \frac{Q'_p}{n} \simeq 5 \left(\frac{Q'_p}{10^6}\right) \left(\frac{M_p}{M_J}\right) \left(\frac{M_*}{M_\odot}\right)^{2/3} \left(\frac{P}{1 \text{ day}}\right)^{13/3} \left(\frac{R_p}{R_J}\right)^{-5} \text{ Myr}, \quad (1)$$

where M_* is the mass of the star, a is the semi-major axis, and n is the orbital mean motion. The derivation of this formula assumes $e \ll 1$ as well as aligned and synchronous planetary rotation, that is, $\Omega_p = n = (GM_*/a^3)^{1/2}$. We will use it as a reference timescale to illustrate

the effects of significant eccentricity and stellar spin.

In Figure 1(b) we plot eccentricity as a function of τ_{ep} of all known planets with $P < 2$ months. The period range in this sample is selected to avoid the observational incompleteness for planets with longer periods. The magnitude of Q'_p is assumed to be 10^6 (see discussions in §2.3). The results in Figure 1(b) clearly show that e is negligibly small (< 0.1) for planets with $\tau_{ep} < 1$ Gyr. In the transition range where $1 \text{ Gyr} < \tau_{ep} < 10 \text{ Gyr}$, planets on circular orbits ($e < 0.1$) coexist with those on eccentric orbits ($e > 0.1$). This dispersion cannot simply be attributed to the difference in the stellar ages (τ_*) since the target stars are chosen for their lack of chromospheric activity which generally indicates $\tau_* \sim$ a few Gyr (see Figure 1(c) for e versus τ_{ep}/τ_*). In addition, their dynamical properties cannot be the main cause because some planets have quite different eccentricities despite the similarity between their periods and mass ratios. Although modest variations in R_p may significantly modify the magnitude of τ_{ep} , planets with $P > 3 - 4$ days cannot be easily inflated by tidally dissipation before their eccentricities are damped out (Gu *et al.* 2003). The insolent effect of stellar irradiation in quenching a planet's Kelvin-Helmholtz contraction (Burrows *et al.* 2000) is also not well correlated with eccentricity (see Figure 1(d) for e versus stellar flux at a). If the short-period planets were scattered to their present location through dynamical instabilities on a variety of timescales, large eccentricities (~ 1) would be expected for all planets with $\tau_{ep} > \tau_*$ and some planets with τ_{ep} smaller than τ_* . This inference is not consistent with the results shown in Figure 1(c). We cannot yet rule out the possibility that the dispersion in the $e - \tau_{ep}$ relation is due to some large-amplitude fluctuations in the Q'_p value which itself may be determined by some stochastic processes (see §2.3).

2.2. Dissipation in the Host Star of the Planetary Tidal Disturbance

The expression in eq(1) does not include the contribution from the dissipation in the star of the planet's tidal disturbance. In the case that both the stellar and planetary spins are aligned with the orbit, the rate of change of e (Eggleton *et al.* 1998, Mardling & Lin 2002) becomes

$$\dot{e} = g_p + g_* \quad (2)$$

where

$$g_{p,*} = \left(\frac{81}{2} \frac{n e}{Q'_{p,*}} \right) \left(\frac{M_{*,p}}{M_{p,*}} \right) \left(\frac{R_{p,*}}{a} \right)^5 \left[-f_1(e) + \frac{11}{18} f_2(e) \left(\frac{\Omega_{p,*}}{n} \right) \right], \quad (3)$$

$$f_1(e) = \left(1 + \frac{15}{4} e^2 + \frac{15}{8} e^4 + \frac{5}{64} e^6 \right) / (1 - e^2)^{13/2}, \quad (4)$$

$$f_2(e) = \left(1 + \frac{3}{2} e^2 + \frac{1}{8} e^4 \right) / (1 - e^2)^5, \quad (5)$$

For $e \ll 1$,

$$g_{p,*} = \left(\frac{81}{2} \frac{n e}{Q'_{p,*}} \right) \left(\frac{M_{*,p}}{M_{p,*}} \right) \left(\frac{R_{p,*}}{a} \right)^5 \left[-1 + \frac{11}{18} \left(\frac{\Omega_{p,*}}{n} \right) \right]. \quad (6)$$

For the case in which only a synchronously spinning planet contributes to \dot{e} , eqs (2) and (6) reduce to eq(1).

Equations (2) and (3) allow us to examine the orbital evolution of star-planet systems with non-synchronized spins and arbitrary eccentricities. For example, a system in which the stellar tide can be neglected, (for instance, if the star were extremely compact), the tidal dissipation in the planet leads to eccentricity excitation if

$$\Omega_p > \Omega_{pc} \equiv \frac{18}{11} f_1(e) n / f_2(e) \rightarrow \frac{18}{11} n \quad (7)$$

as $e \rightarrow 0$ (also see Goldreich & Soter 1966). We now introduce two parameters which characterize the influence of the stellar tide and spin, as well as arbitrary eccentricity, on the orbital evolution of a system. The *eccentricity damping efficiency factor* β is defined as $\beta \equiv \tau_{ep} / \tau_e$, where

$$\tau_e = -\frac{e}{\dot{e}} = \frac{\tau_{ep}}{\beta} \quad (8)$$

is the eccentricity damping timescale. For $\beta < 1$, stellar tides inhibit eccentricity damping, whereas for $\beta > 1$ they enhance the damping rate. Negative values of β corresponds to eccentricity excitation and increasing the eccentricity always enhances the damping rate. From equations (1) to (3) we have

$$\beta = \frac{18}{7} \left\{ \left[f_1(e) - \frac{11}{18} f_2(e) \left(\frac{\Omega_p}{n} \right) \right] + \left[f_1(e) - \frac{11}{18} f_2(e) \left(\frac{\Omega_*}{n} \right) \right] / \lambda \right\}, \quad (9)$$

where

$$\lambda = \left(\frac{Q'_*}{Q'_p} \right) \left(\frac{M_*}{M_p} \right)^2 \left(\frac{R_p}{R_*} \right)^5. \quad (10)$$

Here we have introduced a second parameter, λ , to characterize the importance of the relative masses, radii and Q -values of the star and planet. Generally, tidal dissipation in the planet dominates the evolution when λ is large.

2.3. Magnitude of the Stellar and Planetary Q -values

In eq (10), the value of M_p/M_* can be directly determined from observational data (to within an uncertainty of $\sin i$, where i is the inclination of the system to the line of sight). The value of R_*/R_p can be deduced theoretically from stellar and planetary structure models

or inferred empirically from the observed radius of the transiting planet HD 209458. The major uncertainty is associated with the magnitude of the Q -value because the dominant physical processes which determine the magnitude of $Q'_{p,*}$ in both solar type stars and gas giant planets remain unresolved. Despite the availability of observationally inferred Q -values, it is not clear whether those obtained for solar-type binary stars and for Jupiter (see §1) can be directly applied to hot Jupiters.

Theoretical analyses of tidal evolution mainly focus on the response and dissipation of both equilibrium and dynamical tides. The equilibrium model is based on the concept that a homogeneous spherical body continually adjusts to maintain a state of quasi-hydrostatic equilibrium in the varying gravitational potential of its orbital companion. Internal friction within the body induces the dissipation of energy and a phase lag which gives rise to a net tidal torque which transports angular momentum between the spin of the body and its companion and their orbits. Although turbulence can lead to dissipation in the extended convective envelopes of gaseous giant planets and low-mass stars, the convective turnover timescale is usually much longer than the period of the tidal forcing. Due to this reduction in the efficiency of the turbulent viscosity (Zahn 1977, 1989, Goodman & Oh 1999), the derived rate of angular momentum transfer falls short of that required for the circularization of solar-type binary stars by nearly two orders of magnitude (Terquem et al. 1998). For gas giant planets, turbulent dissipation of equilibrium tides gives $Q \approx 5 \times 10^{13}$ (Goldreich & Nicholson 1977).

In radiative stars, the tidal perturbation of the companion can induce the resonant excitation of low-frequency g-mode oscillations in the radiative region, which carry both energy and angular momentum fluxes (Cowling 1941; Zahn 1970). When this wavelike response is propagated to the stellar surface, radiative damping of the dynamical response provides an effective avenue for tidal dissipation in high-mass binary stars (Savonije & Papaloizou 1983, 1984). However, the envelope of Jupiter is mostly convective (Guillot et al. 2003) and the relevance of g-mode oscillations is less well established (Ioannou & Lindzen 1993a,b, 1994). Nevertheless, the surface layers of hot Jupiters may attain a radiative state because they are intensely heated by their host stars. If so, g-mode oscillations may be excited just above the planet’s convective envelope and dissipated through radiative or nonlinear damping (Lubow, Tout, & Livio 1997) as suggested for high-mass stars (Goldreich & Nicholson 1989). In rotating gaseous planets, Coriolis force can provide a restoring force to the tidal perturbation and induce the resonant excitation of a rich spectrum of inertial modes (Savonije et al. 1995). When the forcing and initial-wave frequencies resonate with each other, the tidal response of the star is greatly enhanced (Papaloizou & Savonije 1997). Hot Jupiters probably formed as rapid rotators such that their tidal forcing occurs in the frequency range of inertial waves, which therefore constitute the natural and dominant response of the planet (Ogilvie & Lin

2004).

In principle, the value of $Q'_{p,*}$ depends in a highly erratic way on the resonant response which is a function of both the planet's spin and the perturber's forcing frequencies as well as the magnitude of viscosity. In the presence of viscosity, the spectrum of inertial waves is discrete, but as the viscosity tends to zero, the spectrum becomes increasingly dense (e.g., Dintrans & Ouyed 2001). In this limit, the dissipation rate may not simply vanish because of the increasing probability of resonant excitation of wave modes. Although the highly variable Q_p values can introduce a dispersion in the rate of eccentricity dissipation, the spin of a planet changes as it undergo Kelvin Helmholtz contraction such that the relevant frequency-averaged Q -value ($\sim 10^6$) may be asymptotically independent of the viscosity in the limit of small Ekman number (Ogilvie & Lin 2004).

Based on these considerations and for computational convenience, we adopt the equilibrium-tide prescription in eq(2) for the determination of the eccentricity evolution of hot Jupiters.

2.4. Eccentricity Evolution of Planets around Rapidly Spinning Stars

The stellar tide can become stronger than the planetary tide if the spin rate of the star is high enough. From eqns(2) and (3) the critical stellar spin rate corresponding to $\dot{e} = 0$ is

$$\Omega_{*c} \equiv \frac{18}{11} \left[(1 + \lambda) \frac{f_1(e)}{f_2(e)} \right] n - \lambda \Omega_p, \quad (11)$$

so that the eccentricity grows if $\Omega_* > \Omega_{*c}$. If $\Omega_p \simeq n$ and $e \ll 1$,

$$\Omega_{*c} = (18 + 7\lambda)n/11. \quad (12)$$

For Jupiter-like planets orbiting solar-like stars, $\lambda = \lambda_{J\odot} \simeq 12$ so that $\Omega_{*c} \simeq 9n$.

In the next section, we show that planets attain a state of synchronization ($\Omega_p = n$) on a timescale (τ_{Ω_p}) which is generally much shorter than that of their host stars (τ_{Ω_*}). We therefore now consider systems in which the planet is nearly synchronously rotating. In Figure 2(a) we plot β (eqn(9)) as a function of stellar spin period for various values of e . For illustration purposes we use $\lambda = \lambda_{J\odot}$ with $Q_p \simeq Q_*$. In addition, we have taken the orbital period to be 6.5 days, representing the three shortest period borderline planets. Now recall that $\beta > 1$ corresponds to enhanced eccentricity damping, $0 < \beta < 1$ corresponds to prolonged circularization times, while $\beta < 0$ corresponds to eccentricity excitation. Also note that stars with radii the same as the Sun's and rotating with velocities $V_r = 50 \text{ km s}^{-1}$ have spin periods of 1 day, while those with $V_r = 10 \text{ km s}^{-1}$ have spin periods of 5 days

(see next section). For each value of Ω_* , β is bounded below by the value corresponding to $e = 0$ (dotted curve). For high values of e , $\beta > 1$ for most stellar spin rates, suggesting that eccentric borderline planets cannot have reached their present positions with eccentricities much higher than presently observed.

Figure 2(b) plots β against Ω_* for the three shortest period borderline systems HD - 168746 ($e = 0.08$, $M_* = 0.92M_\odot$, $M_p \sin i = 0.23M_J$, orbital period $P = 6.4$ days, $\tau_{ep} = 0.60 - 6.0$ Gyr, $\lambda = 127.4$; Pepe et al. 2002), HD 217107 ($e = 0.14$, $M_* = 0.98M_\odot$, $M_p \sin i = 1.30M_J$, $P = 7.1$ days, $\tau_{ep} = 1.90 - 19.0$ Gyr, $\lambda = 7.2$; Fischer et al. 1999), and HD 68988 ($e = 0.15$, $M_* = 1.2M_\odot$, $M_p \sin i = 1.90M_J$, $P = 6.3$ days, $\tau_{ep} = 1.77 - 17.7$ Gyr, $\lambda = 5.0$; Vogt et al. 2002). The ranges for τ_{ep} are calculated using $Q_* = Q_p = 10^5 - 10^6$ to represent the evolution of these parameters. The orbital evolution of HD 168746 was clearly rapid, since any eccentricity greater than its present value would enhance the damping rate even more (see Figure 2(b)). It is likely that the present value is, in fact, much closer to zero. Dissipation within the planet dominated the evolution because the planet-to-star mass ratio is relatively small, and the radii of Saturn-like planets are relatively large (Burrows *et al.* 1997). Taking $R_p = R_{\text{Saturn}} = 0.84R_J$ (and $\sin i = 1$) gives the value for λ quoted above. In contrast, the eccentricity evolution of both HD 217107 and HD 68988 would have been retarded if the stars were rapid rotators initially.

2.5. Dispersion in the Stellar Spin Frequency

The spin frequency of a star is generally believed to be a function of its age, τ_* (see §3). However, in open clusters where member stars presumably have very similar ages, an order of magnitude dispersion has been observed in the stellar rotational velocity. For example, although most G dwarfs in the Pleiades are observed to have rotational speed $V_r \sin i = \Omega_* R_* \sin i < 10 \text{ km s}^{-1}$, at least 20% of them are ultra-fast rotators (UFRs) with $30 \text{ km s}^{-1} < V_r \sin i < 100 \text{ km s}^{-1}$ (Soderblom *et al.* 1993a,b). The spin frequencies of these UFRs exceed the mean motion of planets with periods of several days. (For a star with a solar radius, for example, $V_r = 30 \text{ km s}^{-1}$ corresponding to a spin period $2\pi/\Omega_* = 1.7$ days.) In order to illustrate the importance of stellar spin, we carried out a Monte Carlo simulation in which a sample of planetary candidates was generated with the observed logarithmic period distribution between 3 days and 3 years. By adopting $M_p = 1M_J$, $R_p = 1.35R_J$, $M_* = 1M_\odot$, $R_* = 1R_\odot$, $Q'_p = 10^6$, and $Q'_* = 1.5 \times 10^5$, and taking the planetary spins to be synchronous with the orbital motion, we deduced values for β and τ_e given the observed spin periods of Pleiades stars and the simulated mean motions $n = 2\pi/P$. In Figure 3(a), we plot the inferred values of τ_e/τ_* (the age of the Pleiades cluster is taken to be 7×10^7 yr) for

various simulated values of P . The open circles represent eccentricity damping timescales while the filled dots represent eccentricity excitation timescales. For all planets with $P < 5$ days, the eccentricity is damped on timescales shorter than τ_* . For borderline planets with 5 days $< P < 15$ days, the eccentricities of several systems are damped on timescales $\tau_e > \tau_*$. However, eccentricity is excited for several other systems in this period range. For $P > 15$ days, the eccentricities of most systems are excited on timescales $\tau_e \gg \tau_*$.

Ultra-fast rotators with $V_r \sin i$ up to 200 km s⁻¹ have been observed among the stars of α Persei (Prosser 1992), an open cluster which is younger ($\tau_* \simeq 5 \times 10^7$ yr) than the Pleiades. Although the time available for eccentricity evolution is limited, the relatively small Q'_* values ($\sim 1.5 \times 10^5$ as inferred from observations of binary stars in these young clusters) together with medium to high stellar spin rates imply an enhanced role for the stellar tide and hence retarded eccentricity damping or even eccentricity excitation in some cases. Thus in these young clusters, we expect planets with periods greater than 1-2 days (including those with $\tau_{ep} < \tau_*$) to have a noticeable dispersion in their period-eccentricity distribution.

In older clusters such as the Hyades for which $\tau_* \sim 6 \times 10^8$ yr, $V_r \sin i$ is below 10 km s⁻¹ for nearly all G and K dwarfs. In contrast, most F dwarfs are still fairly rapidly spinning, with rotation speeds in the range 20 – 70 km s⁻¹. We performed a second Monte Carlo simulation, this time for the Hyades, adopting $Q_* = 10^6$ and $\tau_* = 6 \times 10^8$ yr. We found (Figure 3(b)) that the majority of the G and K dwarfs have slowed down sufficiently to promote eccentricity damping of short-period planets. There are nevertheless a few rapidly rotating F dwarfs which continue to promote eccentricity excitation.

2.6. Stellar and Planetary Structural Adjustments

Eqn (2) indicates that \dot{e} is a rapidly increasing function of R_p . The evolution of a and $\Omega_{p,*}$ also depend sensitively on R_p and R_* (see the next section). During the early stages of stellar evolution, both stellar and planetary radii are somewhat larger than their values at later stages. We now assess the effects of stellar and planetary structural adjustment in regulating eccentricity and semi-major axis evolution. For computational convenience, we approximate existing numerical stellar models (Iben 1965, 1967) with the analytic formula

$$R_* \simeq R_\odot (\tau_*/10^7 \text{yr})^{-0.3} \quad (13)$$

for $\tau_* < 10^7$ yr. This timescale for solar-type stars to undergo Kelvin Helmholtz contraction onto the main sequence is much shorter than τ_e or τ_{Ω_*} , such that the initial large stellar radii cannot significantly modify e or Ω_p .

However, planets have much slower Kelvin-Helmholtz contraction rates, (Burrows *et al.* 2000, Bodenheimer *et al.* 2000), and are such that

$$R_p \simeq 1.2R_J(\tau_*/\tau_o)^{-0.1}, \quad (14)$$

where $\tau_o = 1$ Gyr. For $\tau_* = \tau_o$, R_p in this prescription is actually smaller than that used in our models above ($R_p = 1.35R_J$). The larger value takes into account stellar insolation of a short-period planet’s surface, a process which tends to extend its contraction timescale (Burrows *et al.* 2000) and tidal inflation (Bodenheimer *et al.* 2001). Using eqs(2) and (14) for an unheated planet, we find that τ_e is an order of magnitude smaller when $\tau_* = 10^8$ yr than when $\tau_* = 4.6$ Gyr. (For $\tau_* = 10^{7.5-8.5}$ yr, a planet’s size is essentially independent of its mass.) Nevertheless, during the first 10^8 yr, $\tau_e/\tau_* > 1$ and there is insufficient time to circularize the orbits of borderline planets. However, since $\tau_{ep}/\tau_* \propto \tau_*^{-0.5}$, eccentricity damping occurs mostly during the later stages of main sequence evolution and borderline planets can be circularized provided their host stars are not rapid rotators.

In addition to Kelvin Helmholtz contraction, a planet’s size is modified by tidal dissipation which leads to an internal energy generation rate

$$\dot{E}_t = \frac{GM_*M_p e |\dot{e}|_p}{a(1-e^2)} + \alpha_p M_p R_p^2 \Omega_p |\dot{\Omega}_p| \quad (15)$$

where $|\dot{e}|_p$ refers to the planet’s contribution to the circularization process in eq(2) and $\dot{\Omega}_p$ is the rate of change of Ω_p (see next section). For sufficiently large $|\dot{e}|_p$ or $|\dot{\Omega}_p|$, the magnitude of \dot{E}_t exceeds the rate of energy released $\dot{E}_{KH}(M_p, R_p)$ due to an unheated planet’s Kelvin-Helmholtz contraction. In this limit, a planet’s radius evolves toward an equilibrium value R_e such that its surface luminosity, $\mathcal{L}(M_p, R_e)$, is balanced by \dot{E}_t (Bodenheimer *et al.* 2001).

However, the evolution of R_p in eq(14) depends on \dot{E}_{KH} . If a short-period planet arrives at its current location shortly after formation, the value of \dot{E}_{KH} at the time will exceed \dot{E}_t . After that, Kelvin-Helmholtz contraction of the planet will stall once \dot{E}_{KH} becomes less than \dot{E}_t . On the other hand, if a short-period planet acquires its present orbital properties *after* it contracts to a radius $R_p < R_e$, its size will adjust at a rate (Mardling & Lin 2002)

$$\dot{R}_p \simeq \frac{GM_p^2}{R_p \dot{E}_t}, \quad (16)$$

with an enlargement timescale

$$\tau_R = \frac{R_p}{\dot{R}_p} \simeq \frac{M_* R_p}{M_p a} \frac{e^2}{(1-e^2)} \tau_{ep}. \quad (17)$$

This timescale is generally longer than $\tau_{\Omega p}$, in which case a planet cannot inflate significantly before it attains a state of near synchronization (Gu *et al.* 2003).

But, interior to $a \sim 0.04\text{AU}$, $\tau_R < \tau_{ep}$ for a planet with non-negligible eccentricity (> 0.1) so that it can inflate before the eccentricity is damped out. Planetary inflation enhances the rate of tidal dissipation and shortens τ_e . For some values of e and a , R_e exceeds a planet’s Roche radius, $R_R = (M_p/3M_*)^{1/3}a$, so that it begins to lose mass through Roche lobe overflow while its radius is confined to $R_p = R_R$ (Gu *et al.* 2003). Exterior to 0.04 AU, the condition required for planetary inflation ($\tau_R < \tau_{ep}$) is more difficult to satisfy unless the actual eccentricity-damping timescale, τ_e , is significantly prolonged by eccentricity-excitation due to the tidal dissipation inside a rapidly rotating host star, or due to the secular perturbation of other planets. Nevertheless, \dot{E}_t is a rapidly decreasing function of a . Thus for a borderline planet, if a is sufficiently large and \dot{E}_t sufficiently small, R_e is unlikely to be much larger than our adopted values of $1.35 - 1.5R_J$.

2.7. Eccentricity Dispersion Among Borderline Planets

Among the known planets, the shortest period planet with a significant eccentricity is HD 68988, with $e = 0.15$, $P = 6.276$ days, and minimum mass $M_p \sin i = 1.9M_J$. The mass and age of the host star are $M_* = 1.2 M_\odot$ and $\tau_* \simeq 6$ Gyr respectively. Given these values and taking $R_p = 1.35R_J$, $\tau_{ep} \simeq \tau_*$ if $Q'_p \simeq 10^6$ (Vogt *et al.* 2002). The value for R_p is that inferred from transit observations of the short-period planet around HD 209458 (Brown *et al.* 2001).

The dynamical properties of HD 68988 are remarkably similar to those of HD 217107 which has a similar eccentricity ($e = 0.14$). However, there are several other planets such as HD 168746 and HD 130322 which have similar values for τ_{ep} but negligible eccentricities. We propose that the dispersion in eccentricity of borderline planets is correlated with the dispersion of stellar spin frequencies of young stars. Based on the lack of chromospheric activity, Vogt *et al.* (2002) inferred that HD 68988 is a slow rotator. If correct, the stellar tide will be promoting eccentricity damping in this system today. Using the Skumanich law (see eqn (34) below) as well as data from Soderblom *et al.* (1993a, b), we find that the mean spin frequency of F, G, and K stars with an age comparable to that of the Pleiades cluster is about half the present orbital mean motion of the planet around HD 68988, *i.e.* $\Omega_* < \Omega_{pc}$. However, as discussed above, slow and fast rotators coexist in this cluster, with the dispersion in the observed values of $V_r \sin i$ being large. There also exist solar-type stars which are older than the Sun but which are more rapidly spinning. If HD 68988 and HD 217107 were rapid rotators when they were young, at that time $\beta < 1$ so that $\tau_e > \tau_{ep}$ (Figure 2(b)). The effect

of a young star’s tide is also enhanced by its slightly smaller value of Q'_* as inferred from observation. Similarly, if HD 168746 and HD 130322 were slow rotators with $\Omega_* < \Omega_{*c}$ since birth, $\tau_e < \tau_{ep}$.

To support our conjecture, we carried out some numerical simulations using a scheme which calculates the tidal, spin and dynamical evolution of a multi-planetary system (Mardling & Lin, 2002). Using the observed kinematic data for HD 68988 together with $R_p = 1.5R_J$, $R_* = 1.3R_\odot$, $Q'_* \simeq Q'_p \simeq 10^6$, $\Omega_p = n$, and $\Omega_* = 2\pi/(2 \text{ days})$, we obtain $\tau_e \sim \tau_* \sim$ a few Gyr. However, if the spin frequency of the star is halved, τ_e is reduced by a similar factor. The magnitude of τ_e becomes less than 1 Gyr for slowly rotating host stars with $\Omega_* < n$. These numerical results are in general agreement with our conjecture. A more comprehensive numerical analysis is described at the end of the next section.

3. Evolution of the Stellar and Planetary Spins

The above results clearly demonstrate the importance of the stellar tide and spin in the eccentricity evolution of short-period planets. It seems reasonable, therefore, that the dispersion in the $e - \tau_{ep}$ relation is a result of the spread of spins among young stars. However, most of the target stars in the radial velocity surveys are chosen for their low level chromospheric activities. These type of stars, including several borderline systems with measurable eccentricities, have slow rotation speeds like the Sun.

Nevertheless, some, if not all, host stars of extrasolar planets may have been rapidly spinning in the past. It is therefore worthwhile investigating the evolution of Ω_* and Ω_p . Assuming an aligned rotator and that $M_* \gg M_p$, the rate of change of the stellar spin frequency is given by (Mardling & Lin 2002)

$$\dot{\Omega}_* = \frac{9}{2} \left(\frac{n^2}{\epsilon_* \alpha_* Q'_*} \right) \left(\frac{M_p}{M_*} \right)^2 \left(\frac{R_*}{a} \right)^3 \left[f_3(e) - f_4(e) \left(\frac{\Omega_*}{n} \right) \right] + \dot{\omega}_*, \quad (18)$$

where

$$f_3(e) = (1 + \frac{15}{2}e^2 + \frac{45}{8}e^4 + \frac{5}{16}e^6)/(1 - e^2)^6, \quad (19)$$

$$f_4(e) = (1 + 3e^2 + \frac{3}{8}e^4)/(1 - e^2)^{9/2}, \quad (20)$$

and $\dot{\omega}_*$ is the rate of change of the stellar spin due to angular momentum loss via a stellar wind (see the next subsection). The quantity ϵ_* is the stellar mass fraction participating in tidally induced and external angular momentum exchange and α_* is the moment of inertia coefficient of the star. The rate of change of the planet’s spin is given by

$$\dot{\Omega}_p = \frac{9}{2} \left(\frac{n^2}{\epsilon_p \alpha_p Q'_p} \right) \left(\frac{M_*}{M_p} \right) \left(\frac{R_p}{a} \right)^3 \left[f_3(e) - f_4(e) \left(\frac{\Omega_p}{n} \right) \right] + \dot{\omega}_p, \quad (21)$$

where ϵ_p and α_p are the planetary counterparts of ϵ_* and α_* . Note that $\dot{\Omega}_*$ depends more strongly on the mass ratio than does $\dot{\Omega}_p$. Since gaseous planets have extensive convection zones which can be fully mixed, $\epsilon_p \simeq 1$. In contrast, solar-type stars have shallow surface convection zones so that ϵ_* is a few times 10^{-2} for G dwarfs, and an order of magnitude smaller/larger for F/K dwarfs.

3.1. Timescales for Spin and Semi-Major Axis Evolution

The expression for the rate of change of the stellar spin (eq (18)) involves two contributions, as does its counterpart for the rate of change of planetary spin. For post-formation evolution we can neglect $\dot{\omega}_p$ for planets, while $\dot{\omega}_*$ is associated with angular momentum loss via a stellar wind. The tidal transfer of angular momentum induces Ω_p to evolve on a timescale

$$\tau_{\Omega_p} \equiv \left(\frac{n - \Omega_p}{\dot{\Omega}_p} \right)_{\dot{\omega}_p=0} = \frac{7}{2} \alpha_p \left(\frac{R_p}{a} \right)^2 \tau_{ep} \ll \tau_{ep} \quad (22)$$

for non-synchronously spinning planets (see eqns (1) and (18) with $e \ll 1$ and $M_* \gg M_p$). Therefore the planetary synchronization process is much more rapid than the orbital circularization process. However, as a consequence of this, the planetary spin can only be *quasi*-synchronized with the orbit while the eccentricity is non-zero. From eqn (21), this value is $\Omega_p \equiv f_3(e)n/f_4(e) \rightarrow (1 + 6e^2)n$ for $e \ll 1$.

For conservative systems ($\dot{\omega}_* = 0$), the stellar spin evolves on a timescale

$$\tau_{\Omega_*} \equiv \left(\frac{n - \Omega_*}{\dot{\Omega}_*} \right)_{\dot{\omega}_*=0} = \frac{7}{2} \alpha_* \epsilon_* \lambda \left(\frac{M_*}{M_p} \right) \left(\frac{R_*}{a} \right)^2 \tau_{ep} \quad (23)$$

so that for most systems of interest (in the absence of angular momentum loss) we have that $\tau_{\Omega_*} > \tau_{ep}$. Thus we can conclude that Ω_* does not change significantly prior to the circularization of a planet's orbit (in the context of solid satellites around gaseous giant planets, the relative values of τ_{Ω_p} , τ_e , and τ_{Ω_*} are even more extreme because Q' values for satellites are much smaller than those for such planets; Goldreich & Soter 1966). We conclude, therefore, that given the slow stellar rotation rates observed today in borderline systems, were they to have suffered no angular momentum loss in the past, tidal dissipation inside the stars could only ever have enhanced eccentricity damping.

Assuming that the spins of a planet and a star are aligned with the orbit normal of such a system, the total angular momentum perpendicular to the orbit is

$$J_{\text{total}}(a, \Omega_*, e) = J_o(a, e) + J_p(a) + J_*(\Omega_*), \quad (24)$$

where $J_o = M_p a^2 n \sqrt{1 - e^2}$ is the orbital angular momentum. The angular momenta of the planet and star are

$$J_p = \alpha_p M_p R_p^2 \Omega_p \quad (25)$$

and

$$J_* = \alpha_* \epsilon_* M_* R_*^2 \Omega_* \quad (26)$$

respectively, where we have assumed that the whole planet participates dynamically whereas only a fraction ϵ_* of the star is involved in angular momentum exchange. The rate of change of the total angular momentum is

$$\begin{aligned} \dot{J}_{\omega_*} &= \dot{J}_o + \dot{J}_p + \dot{J}_* \\ &= J_o \left(\frac{\dot{a}}{2a} - \frac{e\dot{e}}{1 - e^2} \right) + \alpha_p M_p R_p^2 \dot{\Omega}_p + \alpha_* \epsilon_* M_* R_*^2 \dot{\Omega}_* \end{aligned} \quad (27)$$

where

$$\dot{J}_{\omega_*} = \alpha_* \epsilon_* M_* R_*^2 \dot{\omega}_* \quad (28)$$

is the rate at which the system loses angular momentum via a stellar wind. In a conserved system, we find from Eqns (18) and (21),

$$\frac{1}{2} \frac{\dot{a}}{a} = e\dot{e} - \frac{9}{2} \left\{ \frac{1}{Q'_p} \left(\frac{M_*}{M_p} \right) \left(\frac{R_p}{a} \right)^5 (n - \Omega_p) + \frac{1}{Q'_*} \left(\frac{M_p}{M_*} \right) \left(\frac{R_*}{a} \right)^5 (n - \Omega_*) \right\} \quad (29)$$

to first order in the eccentricity. From Eqns (1) and (8), this can be written as

$$\frac{\dot{a}}{a} = - \left(\frac{2e^2}{\beta} - \sigma \right) / \tau_{ep} \quad (30)$$

where

$$\sigma = \frac{4}{7\lambda} \left(\frac{\Omega_*}{n} - 1 \right) \quad (31)$$

in the limit that $\Omega_p = n$. For small to moderate eccentricities and for most stellar spin periods of interest, as well as for a wide range of star-planet masses and radii (characterized by λ), $|\beta| \sim O(1)$ (Figure 2). However, as illustrated by the shortest period borderline planets described in Section 2.2, λ can vary widely being $\sim O(1)$ for systems with relatively massive planets and lower-mass stars, to several hundreds for systems with lower mass planets and higher mass stars. For systems in which $\Omega_* > n$, $\dot{a} > 0$ as long as $e^2 < \sigma\beta/2$. On the other hand, $\dot{a} < 0$ whenever $\Omega_* < n$.

For Jupiter-mass planets around solar-type stars, $|\dot{J}_p| \ll |\dot{J}_*|$ so that the stellar spin provides the dominant source of angular momentum exchange with the planet's orbit. In

the absence of a stellar wind, stable configurations satisfy $J_o > 3J_*$ (Hut 1980, Lin 1981), or equivalently,

$$a > a_c \equiv \left[\frac{3\alpha_* \epsilon_*}{\sqrt{1-e^2}} \left(\frac{M_*}{M_p} \right) \left(\frac{\Omega_*}{n} \right) \right]^{1/2} R_*, \quad (32)$$

and angular momentum exchange acts to reduce the difference between n and Ω_* until an equilibrium configuration is achieved. The timescale for the semi-major axis to evolve is

$$\tau_a = \frac{a}{|\dot{a}|} = \frac{3}{2} \left(\frac{a}{a_c} \right)^2 \left(\frac{\Omega_*}{|n - \Omega_*|} \right) \tau_{\Omega_*}. \quad (33)$$

3.2. Simultaneous Evolution of the Stellar Spin and Planetary Orbit

Stars are known to lose spin angular momentum via stellar winds so that $\dot{\omega}_*$ in Eqn (18) is finite and negative. The youngest stars are observed to have rapid rotational velocities which are sometimes as high as their breakup speeds (Stassun *et al.* 1999). Although observations of G and K dwarfs in the α Persei and Pleiades clusters (with $\tau_* < 10^8$ yr) indicate a large dispersion in $V_r \sin i$ (with magnitudes ranging from a few to 100-200 km s⁻¹), the same type of stars in the Hyades (with $\tau_* = 6 \times 10^8$ yr) have nearly uniform $V_r \sin i$ which are less than 10 km s⁻¹ (Soderblom *et al.* 1993a,b). The simplest description of the decline in the mean rotation velocity of mature G and K dwarfs is given by Skumanich (1972) such that

$$\langle V_r \sin i \rangle \simeq V_o (\tau_*/\tau_o)^{-0.5} \quad (34)$$

where $V_o \simeq 4$ km s⁻¹ and $\tau_o = 1$ Gyr. A more general description is given by

$$\left(\frac{V_o}{V_r(\tau_*) \sin i} \right)^2 - \left(\frac{V_o}{V_1 \sin i} \right)^2 = \frac{\tau_* - \tau_1}{\tau_o} \quad (35)$$

which more accurately models both the dispersion in V_r among young stars at some initial time τ_1 and the homogeneous low V_r among mature stars with $\tau_* \gg \tau_1$ and τ_o (also see Mayor & Mermilliod 1991 who use a different power index). For G and K dwarfs, $\tau_1 \sim 10^8$ yr and $V_1 \sin i = V_r(\tau_1) \sin i \sim 30$ km s⁻¹. However, the F dwarfs in the Hyades lose very little angular momentum through stellar winds and $V_r \sin i$ continues to extend up to 100 km s⁻¹ at $\tau_* = 6 \times 10^8$ yr. Thus V_o , V_1 , τ_o , τ_1 , and the power indices in eqs (34) and (35) may be functions of M_* .

From the empirical equation (34), we deduce that

$$\dot{\omega}_* = \frac{\dot{V}_r}{R_*} \simeq -\frac{\gamma}{2} \left(\frac{\Omega_o}{\tau_o} \right) \left(\frac{\Omega_*}{\Omega_o} \right)^3 \simeq -\frac{\gamma V_o}{2R_* \tau_o} \left(\frac{\tau_*}{\tau_o} \right)^{-1.5} \quad (36)$$

where differentiation is with respect to τ_* , $\Omega_o = V_o/R_*$ and γ is a calibration factor which is set to unity for G and K dwarfs. Eq(35) yields a similar expression:

$$\dot{\omega}_* \simeq -\frac{\gamma V_o}{2R_*\tau_o} \left(\left(\frac{V_o}{V_1 \sin i} \right)^2 + \frac{\tau_* - \tau_1}{\tau_o} \right)^{-1.5}. \quad (37)$$

In both expressions, the timescale for spin-down induced by a stellar wind is

$$\tau_{\omega_*} \equiv V_r/|\dot{V}_r| \simeq (2\tau_o/\gamma)(\Omega_o/\Omega_*)^2. \quad (38)$$

Due to the initial rapid rate of angular momentum loss, $\tau_{\omega_*} \ll \tau_{\Omega_*}$ for rapidly rotating young G and K dwarfs with τ_* greater than a few times 10^8 yr (i.e the wind-loss timescale is much shorter than the tidally driven synchronization timescales). The evolution of the spin rates of these stars is mainly determined by eq(34) rather than eq(18). However, after these have declined to sufficiently small values, the establishment of a quasi-equilibrium state is possible in which the rate of angular momentum loss via a stellar wind (eq 28) is balanced by the rate at which the star gains angular momentum from the orbit as the planet attempts to spin up the star. Under such circumstances, $\dot{\Omega}_* = 0$ so that from eqn (18) an equilibrium spin rate

$$\Omega_e = \frac{f_3(e)}{f_4(e)} n_e + \frac{2}{9} \left(\frac{\alpha_* \epsilon_* Q'_*}{f_4(e) n_e} \right) \left(\frac{M_*}{M_p} \right)^2 \left(\frac{a_e}{R_*} \right)^3 \dot{\omega}_* \quad (39)$$

is possible provided that

$$|J_{\omega_*}| < \frac{2}{7} \frac{f_3(e)}{\sqrt{1-e^2}} \frac{J_o}{\tau_{ep}}. \quad (40)$$

In eqn (39), a_e is the equilibrium semi-major axis and $n_e = n(a_e)$ is the associated mean motion. This quasi-equilibrium can be established through the evolution of either Ω_* or a so that it is attainable on a timescale given by the minimum of τ_{ω_*} , τ_{Ω_*} , and τ_a . For a given total angular momentum, if $\Omega_p = n$ then the equilibrium quantities of a_e and Ω_e can be determined self-consistently from eqs (39) and (24) as functions of e .

$$J_{\text{total}}(a_e, \dot{\omega}_*, e) = a_e^{9/2} A(e, \dot{\omega}_*) + a_e^{1/2} B(e) + a_e^{-3/2} C(e) \quad (41)$$

where

$$A(e, \dot{\omega}_*) = \frac{2\alpha_*^2 \epsilon_* Q'_* M_*^3 \dot{\omega}_*}{9f_4(e) \sqrt{GM_*} M_p^2 R_*}, \quad (42)$$

$$B(e) = M_p (GM_* (1 - e^2))^{1/2}, \quad (43)$$

and

$$C(e) = \alpha_p M_p R_p^2 \sqrt{GM_*} + \alpha_* \epsilon_* M_* R_*^2 f_3(e) \sqrt{GM_*} / f_4(e). \quad (44)$$

In Figure 4(a), we plot a_e and Ω_e as functions of J_{total} for three values (0, 0.2, 0.5) of the eccentricity. The total angular momentum is normalized by $J_{0.1AU}$, the value of Jupiter’s angular momentum in a $0.1AU$ orbit around the sun. Similar to the calculation presented in Figure 2, we adopt $M_* = 1M_\odot$, $R_* = 1R_\odot$, $M_p = 1M_J$, $R_p = 1.35R_J$, $Q'_p = Q'_* = 10^6$, $\alpha_*\epsilon_* = 0.01$, and $\alpha_p\epsilon_p = 0.2$. However, the establishment of this equilibrium for a wide range in a is only possible for a very slow rate of spin-down, so we set $\dot{\omega}_*$ to be 10^{-4} that in eq(36). In Figure 4(b), we represent a slower spin down rate with the same model parameters except we set ω_* to be one tenth that in Figure 4(a).

The results in Figures 4(a)and 4(b) show that a_e is sensitive to both e and J_{total} , while Ω_e varies primarily with J_{total} . The structures of the curves are indicative of the dominant source of angular momentum in the system, and thus the behavior of the equilibrium is highly sensitive to the planets position. For low eccentricity systems with $a_e > 0.1$, the dominant source of angular momentum is the orbit. Because $\dot{J}_{total} = \dot{J}_\omega < 0$, angular momentum is continually drained from the system, but this only requires minute adjustments to a_e . For low eccentricity systems with $a_e < 0.1AU$ the stellar spin is more prominent and in order to maintain this spin, larger changes in a_e are necessary. When $a_e < 0.1AU$, a planet will move closer to the star as its orbit is circularized, and this will be accompanied by the spin-up of the star. Based on these results (with the planetary and stellar masses and radii given earlier) we infer that as angular momentum is continually lost via stellar winds, the state of near synchronization (in which $\Omega_p = n \simeq \Omega_*$ and $e \simeq 0$) occurs at a semi-major axis of approximately 0.02-0.06 AU and $J_{total}/J_{0.1AU} \approx 1.0$, corresponding to a total angular momentum of approximately $10^{49}g \text{ cm}^2/s$. It is approached asymptotically as J_{total} slowly decreases.

3.3. Present Spins of Host Stars

In general there are two classes of quasi-angular momentum equilibria. The close equilibria with $a_e < a_c$ are unstable to tidally induced angular momentum exchange because they enhance the difference between Ω_* and n and lead to further orbital evolution (Hut 1980, Lin 1981, Rasio *et al.* 1996). There are also those distant equilibria with $a_e > a_c$ which are stable against tidal interaction because they lead to the reduction of difference between Ω_* and n .

The magnitude of a_c does not explicitly depend on J_{total} (see eq 32). However, when the stellar spin equilibrium is attained, its magnitude a_{c0} is determined by Ω_* and n , which along with a_e and J_{total} are functions of e . For the above model parameters, $a_{c0} = 0.029AU$ for $e = 0.2$. We plot the value of a_{c0} and the corresponding J_{total} for various values of e in

Figures 4(a) and 4(b).

The results in these figures also show that a_e is a decreasing function of J_{total} (eq 41). In the large J_{total} limit, if most of the angular momentum is retained by the planet's orbit, a would be large and the rate of tidal transfer of angular momentum would generally be too small to balance the spin down induced by the stellar wind. However, if a large amount of angular momentum is stored in the spin of the planets and their host stars, a small a_e would be sufficient to balance against the large magnitude of \dot{J}_ω . For modest values of J_{total} , it is possible for angular momentum to be mostly contained in the planet's orbit and for the host star to spin relatively slowly with a small magnitude of \dot{J}_ω . In this case, a spin equilibrium can be attained with modest values of a_e . Note that there is an upper limit to the magnitude of a_e ($\sim 0.2 - 0.3\text{AU}$), larger than which the rate of tidal transfer of angular momentum cannot be balanced with the wind loss rate.

The evolutionary fate of planets depends on the magnitude of J_{total} when a reaches a_e . Consider the possibility that a planet has migrated, through its interaction with a nascent disk of gas, residual planetesimals, or other planets, close to the surface of a rapidly spinning host star. If the planet is deposited in a region where Ω_* is smaller than n the planet will not survive. Transfer of angular momentum from the orbit to the stellar spin will cause the planet to migrate into the star. However, if the planet is deposited outside co-rotation ($\Omega_* > n$) its orbit will expand through star-planet tidal interaction while the star spins down through wind losses until the system comes into equilibrium at $a = a_e$. As the star continues to lose angular momentum through its winds, the total angular momentum of the system will decrease and the location of a_e will move inward, as can be seen in Figures 4(a) and 4(b). If the system still retains a relatively large J_{total} (stored primarily in the stellar spin) the magnitude angular momentum lost through winds will be too great for the system to remain in equilibrium. The planet's inward migration would continue until it merges with its host star on a time scale $\tau_a(a_e) < \tau_{\Omega_*}(a_e)$ which, for planets with $P < 2$ days, is less than a few Gyr. However, if a spin equilibrium is retained after J_{total} has already reduced to modest values such that $a_e > a_{c0}$, it would be stabilized against further evolution. Note that the values of a_{c0} correspond to orbital periods in the range of 3-4 days, which are close to the observed cut off in the period distribution of extra solar planets.

In the previous subsection, we indicated that main sequence stars continually lose angular momentum through stellar winds. For example, the ultra fast rotators among the young G and K dwarfs spin down rapidly. During their spin down, the Ω_* of these stars may become comparable to the n of their short-period planets. But this state of near synchronization cannot be maintained because the rate of tidal transfer of angular momentum between a star and its planet, \dot{J}_* , is inadequate to balance that of wind-driven loss of the stellar spin

angular momentum \dot{J}_ω . Consequently, Ω_* reduces to $\Omega_e \ll n$ and a declines through a sequence of non-synchronized (with $\Omega_* < \Omega_s \simeq n$) quasi-equilibria on the timescale of τ_a .

This evolutionary path may have been taken by some G and K dwarf host stars of the shortest-known-period (~ 3 days) planets such as HD 46375 (Marcy *et al.* 2001), HD 177949 (Tinney *et al.* 2001), and HD 187123 (Butler *et al.* 1999). The corresponding V_r for synchronous rotation (with $\Omega_* = n$) in these systems is $\sim 15 \text{ km s}^{-1}$ which is comparable to that of typical dwarf stars in the α Persei and Pleiades clusters (assuming the expectation value $\langle \sin i \rangle = 0.7$). It is entirely possible that some time in the past, the spins of these stars may have been synchronous with the mean motion of their planets. With their present configurations and $Q'_* = 10^6$, their present τ_{Ω_*} of a few Gyr is comparable to their estimated τ_* . Yet the spin of these stars is slow ($\Omega_* < n$), as indicated by their quite chromosphere. We suggest that the effect of the tidal interaction is overshadowed by that of the stellar wind in these G and K dwarfs when they evolved through a state of synchronization. Although they have attained a stable quasi-equilibrium today with $a \sim 2a_c$, their orbit may decay into an unstable configuration with $a < a_c$. In order for these planets to have survived $\tau_* \sim$ a few Gyr, their $\tau_a \sim 2\tau_{\Omega_*} > \tau_*$ which requires Q'_* to be comparable to or greater than 10^6 . In principle, a nearly synchronized quasi-equilibrium (with $\Omega_* \simeq \Omega_s \simeq n$) is attainable for the longer-period (with $P > 10$ days) planets around G and K dwarfs, but the timescale for evolution into such a state is much longer than the age of the mature stars (*i.e.* $\tau_{\Omega_*} \gg \tau_*$) which makes their potential existence coincidental.

But for the more massive F dwarfs, $\tau_{\Omega_*} < \tau_{\omega_*}$ because their $\dot{\omega}_*$ is much smaller than that of the G and K dwarfs. For these stars, we can use eq (36) for $\dot{\omega}_*$ by setting $\gamma \sim 0.1$. In this case, the state of quasi-equilibrium may be maintained because the transitory decline of Ω_* can be compensated by a tidal transfer of angular momentum from the planet's orbit to the stellar spin, resulting in a net increase in both Ω_e and $n(a_e)$ and a reduction in a_e . In addition, the relatively shallow convection zone of the F dwarfs also reduces their ϵ_* and a_c well below that of the G and K dwarfs. It is thus possible to attain a sequence of nearly synchronized (with $\Omega_* \simeq \Omega_s \simeq n$) quasi equilibria with $a_e > a_c$. This sequence of events may have led to the present orbital configuration of the planet around τ Boo.

3.4. Numerical Models of Spin-Orbit Evolution

In order to verify the above qualitative and analytic description, we numerically integrate, with a fourth-order Runge-Kutter scheme, eqs (2), (18), (21), and (30) with appropriate substitutions for $f_{1,2,3,4}$, $\dot{\omega}_*$, $\dot{J}_{p,*}$. The dependent variables are $\Omega_{p,*}$, a , and e . We adopt the standard model parameters in which $M_* = 1M_\odot$, $M_p = 1M_J$, $R_* = 1R_\odot$, $R_p = 1.5R_J$,

$\dot{\omega}_p = 0$, and $Q'_p = 10^6$. Assuming that Q'_* is around 1.5×10^5 before $t = 10^8$ yr and 10^6 after $t = 10^9$ yr, the star's dissipation parameter is taken to be of the form $Q'_* = a + b \operatorname{erf}[(\tau' - 5)/3]$, where $\tau' = t/10^8$ yr, $a = 5.75 \times 10^5$ and $b = 4.2 \times 10^5$.

In order to demonstrate several possible outcomes, we constructed six models. In models 1 and 2, we set $P = 3$ days at $t = 0$ to represent the shortest period planets. In models 3 and 4, P is set to be 7 days at $t = 0$ as a possible initial condition of borderline planets. In models 5 and 6, we choose $P = 1.5$ days to represent some hypothetical ultra-short-period planets which may have once existed close to the surface of their host stars. To explore the effects of stellar spin, models 1, 3, and 5 start with $\Omega_* = 10n$, while in models 2, 4, and 6, $\Omega_* = 9n$. These spin rates are rapid, but not near the break up values. In all models, we choose $\Omega_p = 10n$ and $e = 0.2$ at $t = 0$. All models are integrated for 6 Gyr.

In Figure 5(a), we plot the e evolution of models 1, 2, 3, and 4 which are represented with solid, short-dashed, long-dashed, and dot-dashed lines respectively. Both models 5 and 6 are represented by dotted lines. In Figures 5(b), 5(c), and 5(d), we plot the evolution of a , Ω_p/n and Ω_*/n respectively.

After brief initial episodes of e excitation, e declines rapidly in models 1, 2, 5, and 6. Close to the star, $\tau_e \approx 3$ Gyr for the short-period planets, and rapid late stage e damping erases any trace of early e excitation. Despite an initial decline in the eccentricities in models 5 and 6, the planet migrates outward and e levels off. Eventually it is caught at in the quasi-equilibrium at a_e , and e begins to drop again. In models 3 and 4, the eccentricity is maintained at non-zero values even after 6 Gyr. The contrasts seen in the models with different stellar spin rates supports our conjecture that the dispersion in the $e-P$ distribution may be due to tidal dissipation in host stars with various rotation speeds.

The planets quickly decrease in spin frequency due to the artificially high initial values. They are all able to attain synchronous spin frequency within $\sim 1 - 2$ Gyr, with the closer planets doing so more quickly. The effect of the stellar spin on planetary spin is negligible.

After 400–500 Myr, all the models are caught in the quasi-equilibrium described earlier in this paper. As angular momentum is lost to stellar-winds it is balanced by tidal transfer from the orbit to the star. Both the semi-major axis and stellar spin reach their equilibrium values described by eq (39), eq (41) and shown in Figure 4. Models 2, 4, and 6, that start with slower initial stellar spins, have correspondingly smaller equilibrium stellar spins and semi-major axes. Any subsequent evolution proceeds on much longer timescales governed by $\dot{\omega}_*$.

In all the models the stellar spin steadily decreases from a large initial value. However, Figure 5(d) reflects changes in both stellar spin and semi-major axis. The stellar spin in

model 1 initially decreases more quickly than the orbital frequency, but by ~ 100 Myr the orbital frequency is decreasing faster and Ω_*/n increases. The same behavior occurs in model 5, but at an earlier time. Models 3 and 4 have such large semi-major axes that the stellar spin must decrease significantly before any equilibria can be established. In Models 3, 4, 5, and 6 the stellar spin has stopped changing by the time the semi-major axis reaches its equilibrium value. In contrast, the stellar spin in models 1 and 2 continues to decrease for about 100 Myr, even after the semi-major axis has stopped changing significantly. Further evolution should slowly move the system from quasi-equilibrium into synchronization ($\Omega_p = n \simeq \Omega_*$ and $e \simeq 0$).

4. Summary and Discussion

In this paper we have considered the effect of tidal interaction between main sequence dwarf stars and their short-period planets. It is generally customary to assume that the orbital eccentricity of planets is primarily damped by the dissipation of stellar tidal disturbance inside the planets. Such a scenario provides a reasonable account for the circular orbits of planets with periods less than about a week. But for planets with periods slightly longer than a week, there is a spread of orbital eccentricity. We suggest that this dispersion is associated with different past rotational speed and a range of spin down rate among their host stars. This conjecture can be best verified by the detection of short-period planets around stars in young clusters such as α Persei and Pleiades. We expect short-period planets around rapidly rotating F, G, and K dwarfs to have relatively large eccentricities. For older clusters such as the Hyades, short-period planets around F dwarfs should have larger eccentricities than those around G and K dwarfs, mainly due to the difference in the stellar spin-down rate.

Rapid stellar spin also causes outward orbital migration on slightly longer timescales. Thus we expect the minimum orbital period for planets around rapidly rotating dwarfs in young clusters to be less than its present 3 day value. In contrast, this cutoff period for slowly rotating dwarfs in young clusters should be the same as its present value. It is also possible that the period cutoff represents the boundary corresponding to survivability against tidally induced orbital decay. In that case, the period cutoff for slowly rotating dwarfs in young clusters would be shorter than 3 days.

During their spin down, the stars' spin angular frequency temporarily coincides with the mean motion of the planets. Among the short-period systems, this state of near synchronous rotation can only be preserved around F dwarfs which spin down gradually. All main sequence dwarfs attain a quasi-angular momentum equilibrium in which the host stars' loss of angular momentum through stellar winds is balanced by their tidal transfer of angular

momentum with their planets. For G and K dwarfs, the equilibrium frequencies are much smaller than that for F dwarfs. Consequently, it is much easier to form short-period nearly synchronous systems around F dwarf than around G and K dwarfs.

Despite the enormous progress that has been made in the area of extra solar planet searches, there is insufficient data to verify our conjecture. But future radial-velocity, astrometric, and transit searches for planets in clusters of various ages should provide sufficient data to test the scenario presented here.

We thank D. Fischer, P.G. Gu, S. Martell, and L. Langland-Shula for useful conversations. D. Lin thanks the director, D.O. Gough, of the Institute of Astronomy, Cambridge University for hospitality while some of this work was completed. This research has been supported in part by the Sackler Foundation, NSF through grants AST-9987417, by NASA through grants NAG5-7515, NAG5-8196, and NAG5-10727, an astrophysics theory program which supports a joint Center for Star Formation Studies at NASA-Ames Research Center, UC Berkeley, and UC Santa Cruz, and by the Victorian Partnership for Advanced Computing.

- Artymowicz, P. 1992, *PASP*, 104, 769
- Bodenheimer, P., Lin, D.N.C. & Mardling, R.A. 2001, *ApJ*, 548, 466
- Brown, T. M., Charbonneau, D., Gilliland, R. L., Noyes, R. W., Burrows, A. 2001, *ApJ*522, 699
- Burrows, A., Guillot, T., Hubbard, W. B., Marley, M. S., Saumon, D., Lunine, J. I. & Sudarsky, D. 2000, *ApJ*, 534, 97
- Burrows, A., Marley, M., Hubbard, W. B., Lunine, J. I., Guillot, T., Saumon, D., Freedman, R., Sudarsky, D. & Sharp, C. 1997, *ApJ*, 491, 856
- Butler, R. P., Marcy, G. W., Vogt, S. S., Apps, K. 1998, *PASP*, 110, 1389
- Butler, R.P., Marcy, G.W., Fischer, D.A., Brown, T.M., Contos, A.R., Korzennik, S.G., Nisenson, P. & Noyes, R.W. 1999, *ApJ*, 526, 916
- Cowling, T. G. 1941, *MNRAS*, 101, 367
- Dintrans, B., & Ouyed, R. 2001, *A&A*, 375, L47
- Eggleton, P.P., Kiseleva, L.G., Hut, P. 1998, *ApJ*, 499, 853
- Fischer, D.A., Marcy, G.W., Butler, R.P., Vogt, S.S. & Apps, K. 1999 *PASP*, 111, 50
- Goldreich, P., & Nicholson, P. D. 1977, *Icarus*, 30, 301
- Goldreich, P., & Nicholson, P. D. 1989, *ApJ*, 342, 1079
- Goldreich, P. & Sari, R. 2003, *ApJ*, 585, 1024
- Goldreich, P. & Soter, S. 1966, *Icarus*, 5, 375
- Goldreich, P., & Tremaine, S. 1980, *ApJ*, 241, 425
- Goodman, J. & Oh, S. P. 1997, *ApJ*, 486, 403
- Gu, P.G., Lin, D.N.C., & Bodenheimer, P. 2003, *ApJ*, 588, 509
- Gu, P.G., Bodenheimer, P. & Lin, D.N.C. 2004, *ApJ*, 608, 1079
- Guillot, T., Hubbard, W. B., Stevenson, D. J., & Saumon, D. 2004, in *Jupiter*, ed. F. Bagenal, F., T. Dowling, & W. McKinnon (Cambridge: Cambridge Univ. Press), in press
- Hut, P. 1980, *Astron. Astrophys.*, 92, 167
- Iben, I. 1965, *ApJ*, 141, 993

- Iben, I. 1967, *ApJ*, 147, 624
- Ioannou, P. J., & Lindzen, R. S. 1993a, *ApJ*, 406, 252
- Ioannou, P. J., & Lindzen, R. S. 1993b, *ApJ*, 406, 266
- Ioannou, P. J., & Lindzen, R. S. 1994, *ApJ*, 424, 1005
- Lin, D. N. C. 1981, *MNRAS*, 197, 1081
- Lin, D. N. C., Bodenheimer, P., & Richardson, D. C. 1996, *Nature*, 380, 606
- Lubow, S. H., Tout, C. A., & Livio, M. 1997, *ApJ*, 484, 866
- Marcy, G. W., Butler, R. P., & Vogt, S. 2000a, *ApJ*, 536, 43
- Marcy, G. W., Butler, R. P., Williams, E., Bildsten, L., Graham, J. R., Ghez, A. M., & Jernigan, J. G. 1997, *ApJ*, 481, 926
- Marcy, G. W., Cochran, W. D., & Mayor, M. 2000, in *Protostars and Planets IV*, ed. V. Mannings, A. P. Boss & S. S. Russell (Tucson:Univ. of Arizona Press), 1285
- Mardling, R.A. & Lin, D.N.C. 2002, *ApJ*, 573, 829
- Mathieu, R. D. 1994, *ARA&A*, 32, 465
- Mayor, M. & Mermilliod, J.C. 1991 in *Angular Momentum Evolution of Young Stars*, eds S. Catalano & J.R. Stauffer, (Dordrecht: Kluwer), 143
- Murray, C. D. & Dermott, S. F. 1999, *Solar System Dynamics*, Cambridge University Press, Cambridge
- Murray, N., Hansen, B., Holman, M. & Tremaine, S. 1998, *Science*, 279, 69
- Ogilvie, G.I. & Lin, D.N.C. 2004, *ApJ*, 610, 477
- Papaloizou, J.C.B., Nelson, R.P. & Masset, F. 2001, *Astron. Astrophys.*, 366, 263
- Papaloizou, J. C. B., & Savonije, G. J. 1997, *MNRAS*, 291, 651
- Peale, S. J. 1999, *ARA&A*, 37, 533
- Pepe, F., Mayor, M., Galland, F., Naef, D., Queloz, D., Santos, N., Udry, S. & Burnet, M. 2002, *A&A*, 388, 632
- Prosser, C.F. 1992, *AJ*, 103, 488
- Rasio, F. A., & Ford, E. B. 1996, *Science*, 274, 954

- Rasio, F. A., Tout, C. A., Lubow, S. H., & Livio, M. 1996, *ApJ*, 470, 1187
- Savonije, G. J., & Papaloizou, J. C. B. 1983, *MNRAS*, 203, 581
- Savonije, G. J., & Papaloizou, J. C. B. 1984, *MNRAS*, 207, 685
- Savonije, G. J., Papaloizou, J. C. B., & Alberts, F. 1995, *MNRAS*, 277, 471
- Skumanich, A. 1972, *ApJ*, 171, 565
- Soderblom, D., Stauffer, J., Hudon, J.D. & Jones, B. F. 1993a *ApJS*, 85, 315
- Soderblom, D., Stauffer, J., MacGregor, K. B. & Jones, B. F. 1993b *ApJ*, 409, 624
- Stassun, K., Mathieu, R., Mazeh, T. & Vrba, F. 1999, *AJ*, 117, 2941
- Terquem, C. , Papaloizou, J. C. B. , Nelson, R. P. , & Lin, D. N. C. 1998, *ApJ*, 502, 788
- Tinney, C. G., Butler, R. P., Marcy, G. W., Jones, H. R. A., Penny, A. J., Vogt, S. S., Apps, K., Henry, G.W. 2001, *ApJ*, 551, 507
- Trilling, D. E. 2000, *ApJ*, 537, 61
- Trilling, D. E. , Benz, W. , Guillot, T. Lunine, J. I. , Hubbard, W. B. , & Burrows, A. 1998, *ApJ*, 500, 428
- Vogt, S.S., Butler, R.P, Marcy, G.W., Fischer, D.A., Pourbaix, D., Apps, K. & Laughlin, G. 2002, *ApJ*, 568, 352
- Yoder, C. F., & Peale, S. J. 1981, *Icarus*, 47, 1
- Zahn, J.-P. 1970, *A&A*, 4, 452
- Zahn, J.-P. 1977, *A&A*, 57, 383
- Zahn, J.-P. 1989, *A&A*, 220, 112

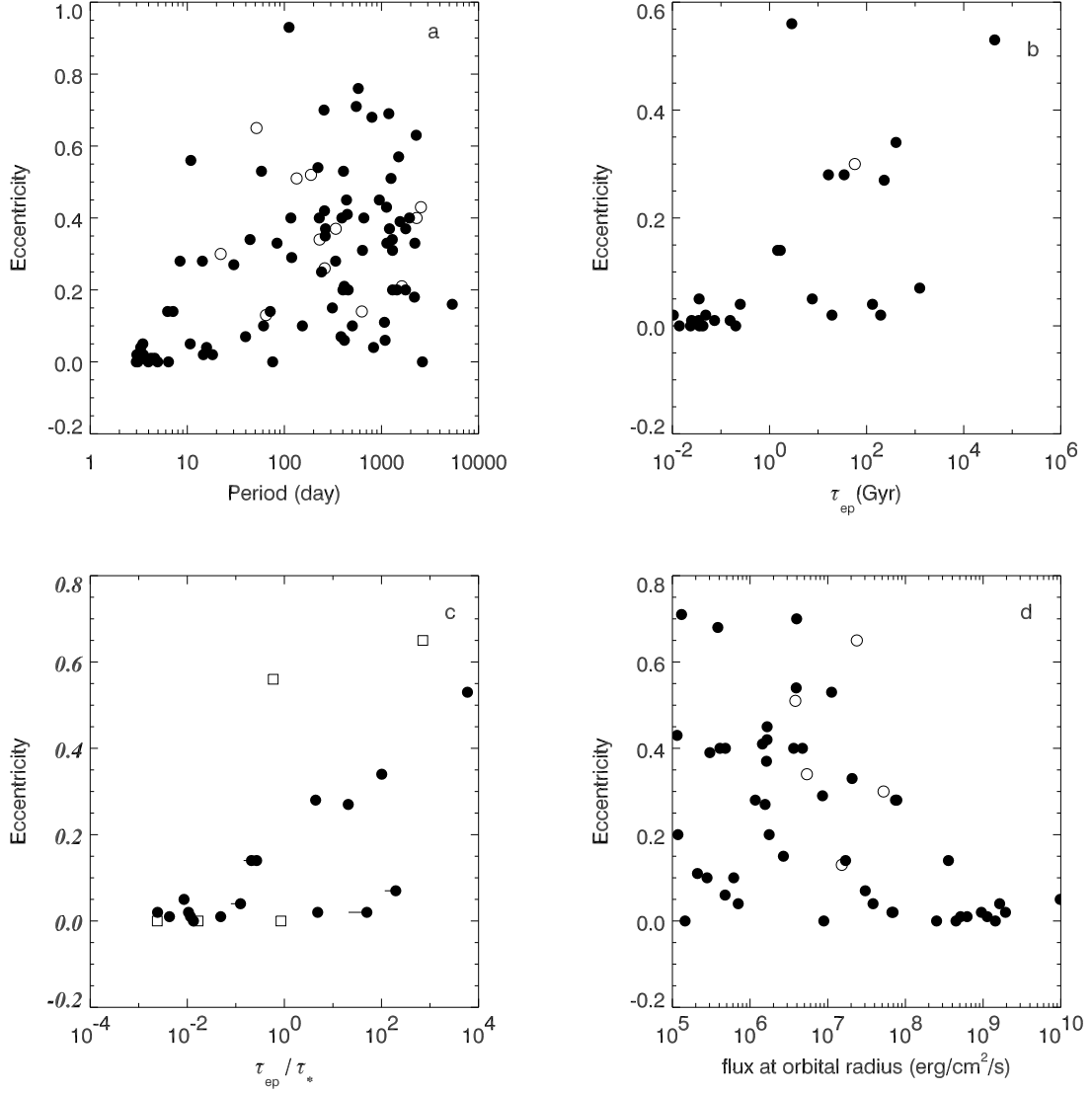


Fig. 1.— (a) Period-eccentricity relation for extrasolar planets, (b) Eccentricity as a function of eccentricity-damping timescale for planets with orbital periods less than two months, (c) Eccentricity as a function of eccentricity-damping timescale normalized by the stellar age, (d) Eccentricity as a function of stellar flux received at planets orbital radius.

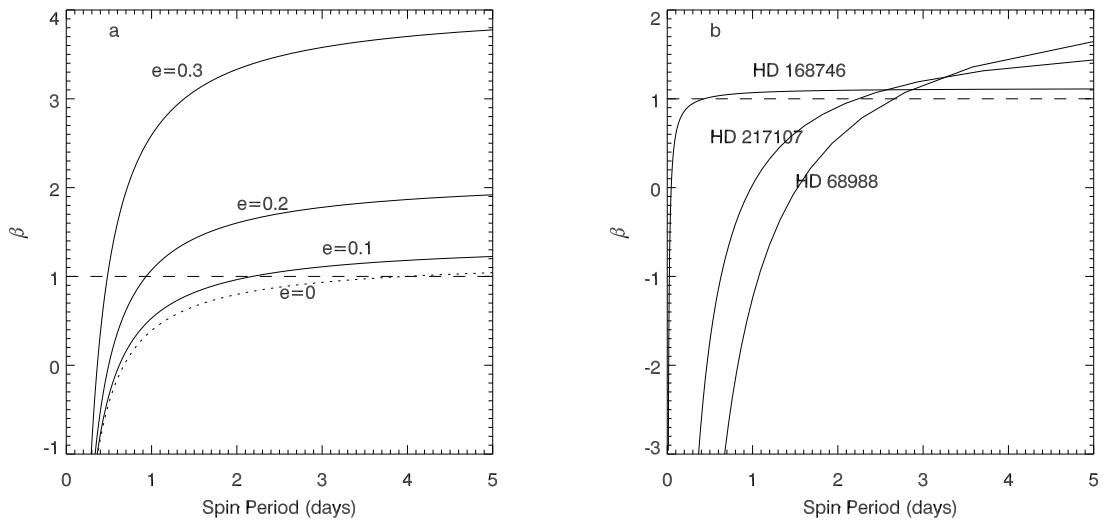


Fig. 2.— Eccentricity damping efficiency factor β vs. stellar spin period. (a) Sun/Jupiter parameters with $Q_* = Q_p$, $P = 6.5$ days and various eccentricities. (b) Three representative borderline systems.

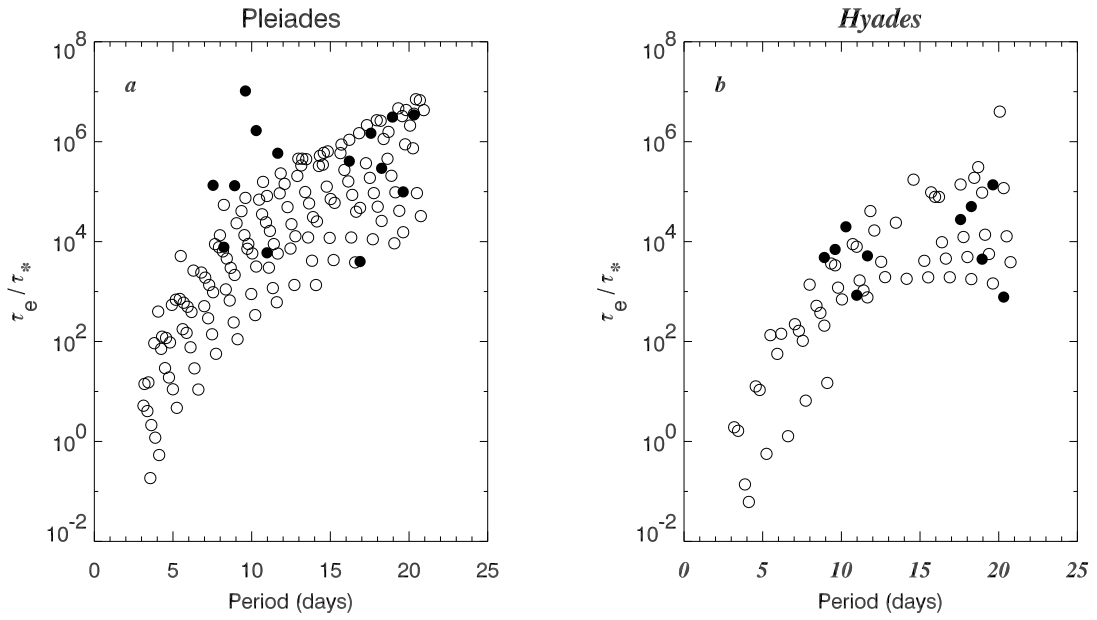


Fig. 3.— τ_e/τ_* for stars as a function of orbital period. Empty circles correspond to eccentricity damping and filled circles are excitation timescales. (a) Pleiades cluster ($\tau_* = 70Myr$). (b) Hyades cluster ($\tau_* = 600Myr$). τ_e was calculated assuming planet-orbit synchronization and eccentricities between 0.0 and 0.7 (see text for more details).

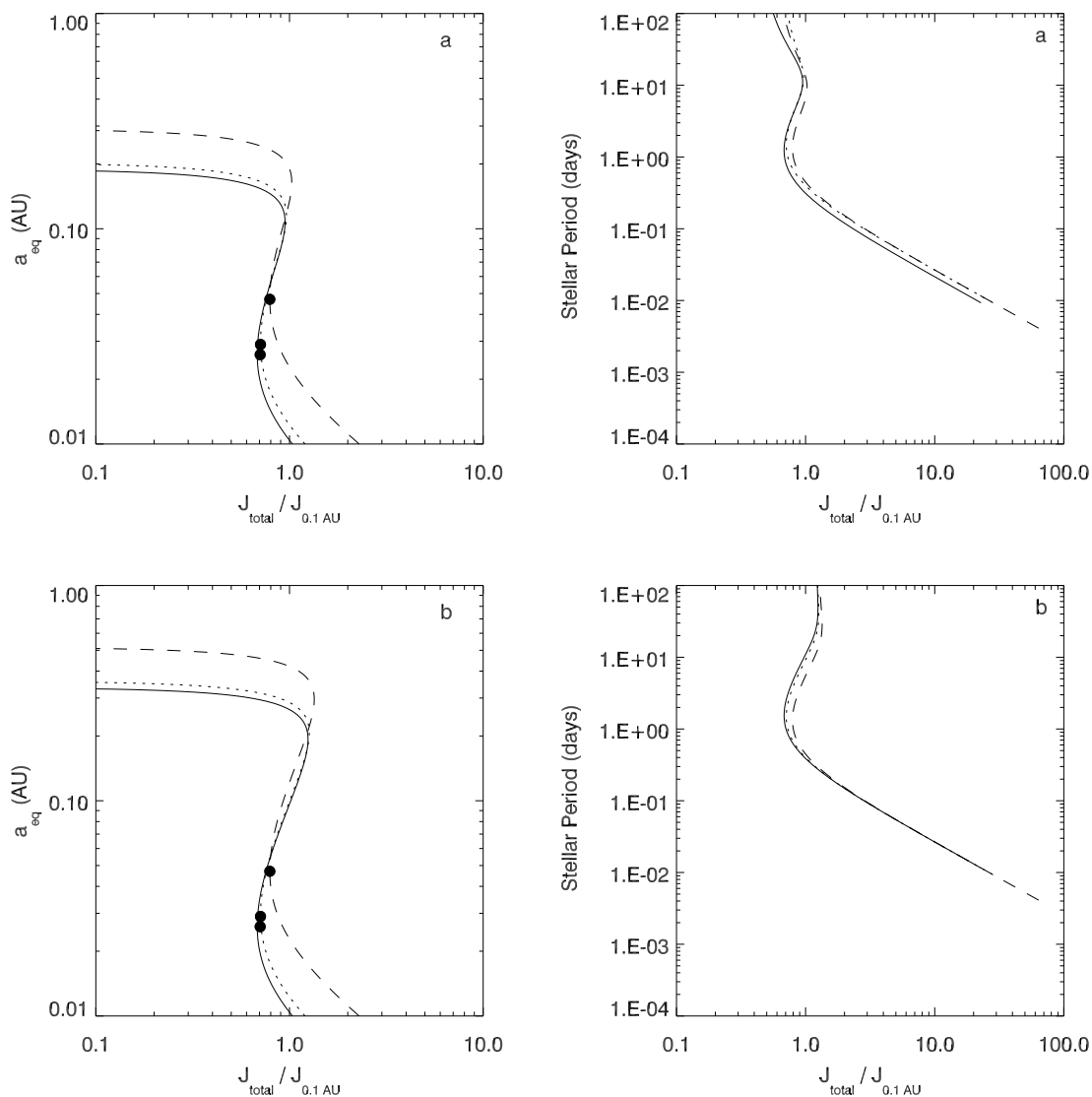


Fig. 4.— (a) The equilibrium semi-major axis and stellar spin period as a function of total angular momentum in the system for three eccentricities: $e=0$ (solid), $e=0.2$ (dotted), and $e=0.5$ (dashed). The equilibrium is reached when the angular momentum lost to stellar winds is balanced by that transferred from the orbit and spin of the planet such that the stellar spin remains constant. (b) Stellar wind set at one-tenth that in (a).

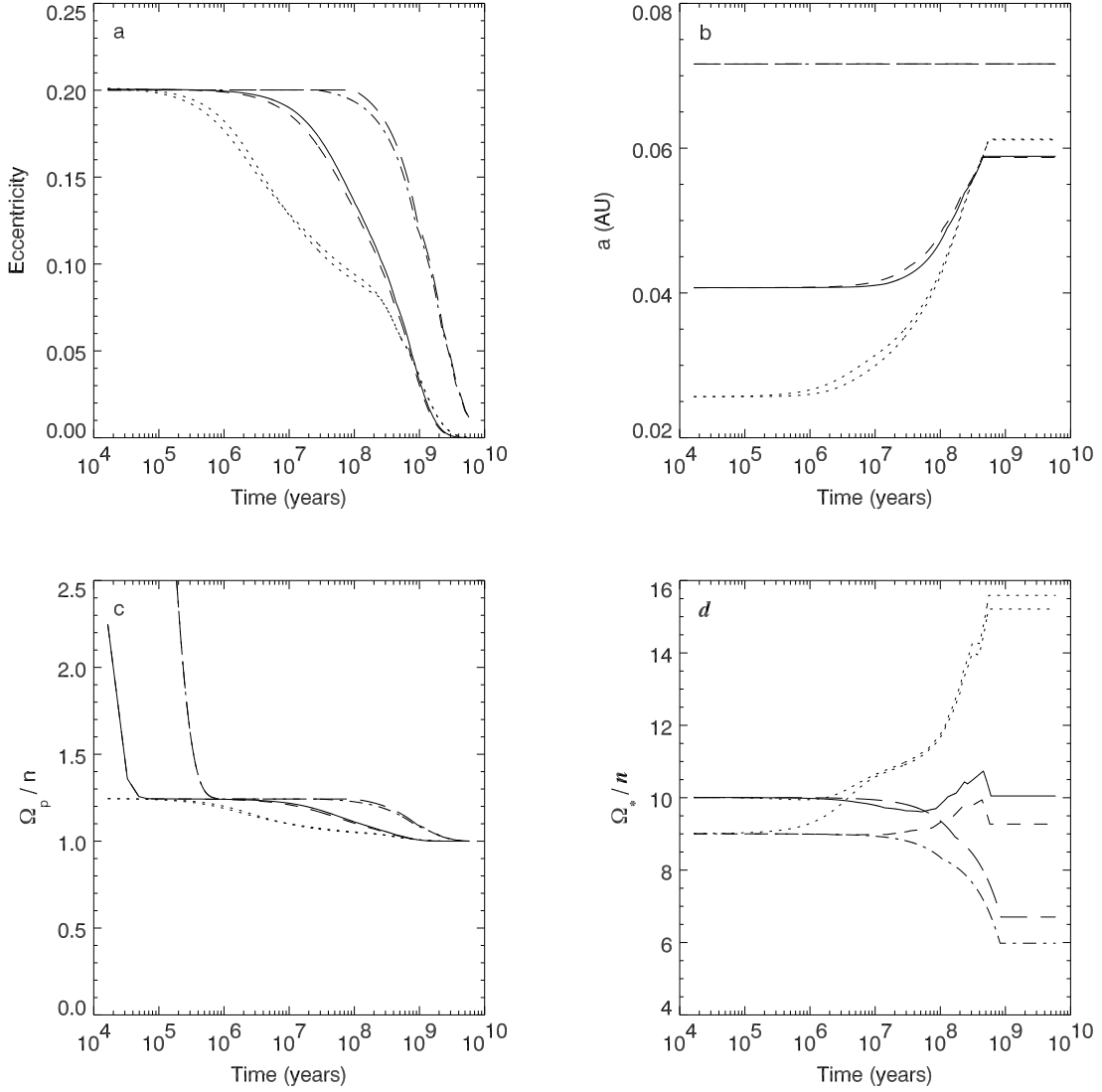


Fig. 5.— Results of a long-term integration of eccentricity, semi-major axis, stellar spin frequency and planetary spin frequency. Models 1, 2, 3, and 4 are represented with solid, short-dashed, long-dashed, and dot-dashed lines respectively. Models 5 and 6 are represented with dotted lines. (a) Eccentricity as a function of time, (b) Semi-major axis as a function of time, (c) Ratio of planetary spin to orbital frequency as a function of time, (d) Ratio of stellar spin to orbital frequency as a function of time.